

INFLUENCE OF THE PRESSURE DIE GEOMETRY ON THE BENT TUBE OVALITY

JAN RIHACEK, MICHAELA CISAROVA, EVA PETERKOVA, KAMIL PODANY

Brno University of Technology, Faculty of Mechanical Engineering, Institute of Manufacturing Technology, Brno, Czech Republic

DOI : 10.17973/MMSJ.2021_6_2021082

e-mail: rihacek.j@fme.vutbr.cz

The paper deal with analysis and optimization of the pressure bar geometry in the case of the tube bending. The bending process is realized on Wafios RBV 60 ST CNC bending machine using rotary draw bending system. The processed semi-finished product is a tube, which is made of 24MnB5 steel. Currently, after tube bending by an angle of 120°, an unacceptable ovality occurs on its body. Therefore, the article presents the optimization of the pressure bar geometry, which helps to prevent the occurrence of the mentioned defect. Due to the least possible intervention in the bending process, only the change in the pressure bar geometry is tested. For this reason, a numerical simulation in ANSYS software is performed. Before the actual optimization, an accuracy of the simulation is verified by comparing the real initial state with simulation results.

KEYWORDS

Finite element analysis, numerical simulation, ANSYS, 34MnB5 steel, tube bending

1 INTRODUCTION

One of the reasons for focusing on the area of tube bending is mainly the current trend of reducing the weight of parts. Bending is the primary technology of sheet metal forming, through which the desired shape is achieved not only of tubular parts or pipes, but also of profiles, bars or sheets.

One of the most common and universal methods to bend tube is rotary draw bending (RDB). Tubes with a diameter of 12 to 250 mm are usually bent to a bending angle of up to 180° by mentioned method. RDB also allows the bending of very small radii (approaching to the tube diameter), even thin-walled tubes. However, the prerequisites are adequate tools, which guarantee the repeatability of production. Basically, the bending is realized by rotating bend die, to which the tube is attached by means of a clamp die. During the bending operation, the pressure bar forces the tube into the groove of the bend die, so it can be formed, see schematic view in Fig. 1.

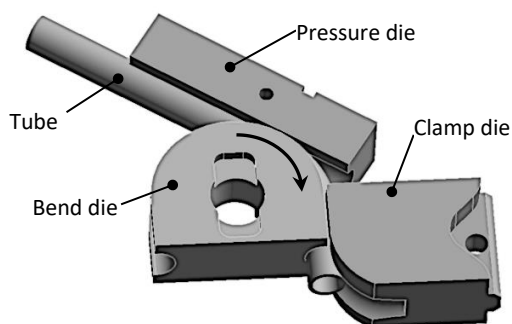


Figure 1. Basic principle of RDB

The pressure die can be fixed in place or movable during the bending process. In the case of the die movement alongside the tube, it can be also called as a boosting, which provides better guidance and eliminates wear on the contact surfaces against the fixed pressure bar.

Principal problems in the tube bending process are associated with occurrence of different defects, which is an inevitable phenomenon in practice. Parameters such as tool geometry, material, chosen bending technology, or tool wear have an important role in the formation of defects. The most common defects in the tube bending process include cross-section flattening – ovality, wall thinning, wall wrinkling or enormous springback. However, it should also be noted that many defects are an accompanying phenomenon during bending and they cannot always be eliminated.

1.1 Tube Ovality and Possibilities of its Reduction

One of the basic and most common defects is the ovality of the bent tube cross-section. The force effects of tools during bending cause the deformation of the originally circular shape of the tube cross-section with diameter D_0 . Therefore, its flattening occurs, as can be seen in Fig. 2.

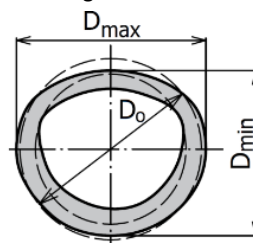


Figure 2. Cross-section ovality [Srom 2017]

Ovality can be described on the basis of several possible relationships, most often on the basis of the so called ovality coefficient. In many cases, it is defined by manufacturing companies or their customers. The same applies to defining the permissible values of the coefficient. Equation (1) gives one of the possible approach to determination of the ovality coefficient:

$$K_O = \frac{D_{max} - D_{min}}{D_0} \cdot 100 \quad (1)$$

where K_O is the ovality coefficient [%], D_{max} is the maximum cross-sectional dimension [mm], D_{min} is the minimum cross-sectional dimension [mm], D_0 is the initial tube diameter [mm].

For the description of the ovality origin, it is necessary to introduce a suitable coordinate system, from which the indexing of directions is based. Effects acting in the longitudinal direction are indicated by the index "x", in the circumferential direction "c" and the radial direction as "r". The tube is mostly stressed in the longitudinal direction by a stress σ_x under the action of a bending moment "M_o". By limiting the action of stress on the set element, force effects in the longitudinal direction F_x are obtained, as can be seen from Fig. 3. The forces act in both directions. Their superposition gives a force resultant directed to the bending axis. Due to the bending moment, compressive and tensile stresses are created in the cross section of the tube. On the outer radius of bending, there is a longitudinal tensile stress, while a longitudinal compressive stress is on the inner radius. The tangential stress has a compressive effect throughout the tube circuit. Since the wall thickness is several times smaller than the tube diameter, the radial stress σ_r can be neglected. [Li 2010], [Liu 2011]

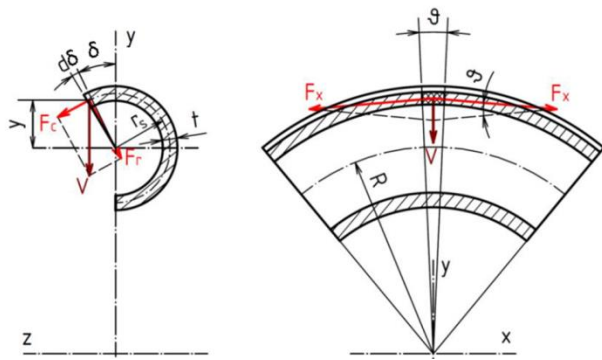


Figure 3. Force distribution on the bent tube [Srom 2017]

In the cross-section plane, the dependence of the circumferential stress on the longitudinal stress can then be expressed as:

$$\sigma_c = -\sigma_x \cdot \frac{1 - \cos\delta}{2 \cdot \frac{R}{2r} + 1} \quad (2)$$

where σ_c is the circumferential stress [MPa], σ_x is the longitudinal stress [MPa], δ is the angle of the element position in the cross section [°], R is the bending radius [mm] and r is the tube diameter [mm].

Assuming consideration of maximum shear stress theory, the relation between circumferential and longitudinal stresses is also given for outer cross-section semicircle (3) and inner semicircle (4) as:

$$|\sigma_x| + |\sigma_c| = \sigma_k \quad (3)$$

$$|\sigma_x| - |\sigma_c| = \sigma_k \quad (4)$$

where σ_k is the yield strength [MPa].

Then, the longitudinal stress can be expressed using the following equation:

$$\sigma_x = \sigma_k \cdot \frac{2 \cdot \frac{R}{2r} + 1}{2 \cdot \frac{R}{2r} + 2 - \cos\delta} \quad (5)$$

Consequently, the longitudinal stress is tied to a force reaction F_x . However, by acting of the axial force components F_x , a reaction is occurred in the base of the radial force F_r , which in turn causes flattening of the cross-section called ovality, because the radial force components always act against each other around the circumference of the bent cross-section, as it is better shown in Fig. 4. [Ghafoor 2001], [Safdarian 2019]

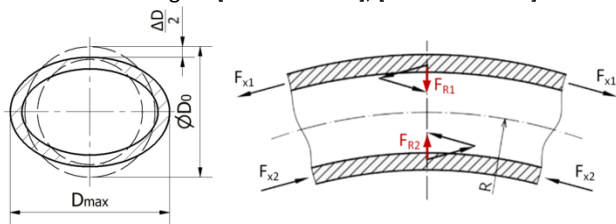


Figure 4. Force decomposition at the bending point [Wello 2015]

The analytical approach [Tang 2000] gives the equation for determining the reaction force by equation (6) and also a simplified condition for ovality origin (7) depending on the bending radius, thickness and inner radius of the tube cross-section.

$$F_R = \sigma_k \cdot r \cdot \frac{\pi}{2} \cdot t \cdot \frac{\xi}{R} \quad (6)$$

where t is the wall thickness [mm] and ξ is the thin ring of thickness ($\xi = R \cdot \vartheta$) [mm].

$$R \leq \frac{3.43 \cdot r^2}{t} \quad (7)$$

Various authors have in the past tried to derive an analytical solution to the degree of ovality. For example, the literature [Welo 2015] determines ovality simply as a symmetrical flattening (see Fig. 4), based on the consideration of Hollomon's hardening law for the tube material:

$$\sigma = K \cdot \varphi^n \quad (8)$$

where σ is the flow stress [MPa], K is the strength coefficient [MPa], φ is the true strain [-] and n is the strain hardening coefficient [-].

Then the value of symmetrical flattening is given as:

$$\Delta D = \frac{9}{64} \cdot \frac{D_s^5}{R^2 \cdot t^2} \cdot \left(\frac{2 \cdot R \cdot b}{D_s} \right)^n \cdot \left[\frac{\sqrt{\pi}}{(n-3)} \cdot \frac{\Gamma\left(1-\frac{n}{2}\right)}{\Gamma\left(\frac{1}{2}-\frac{n}{2}\right)} - \frac{n}{(n-2) \cdot (n-4)} \right] \quad (9)$$

where D_s is the mean tube diameter [mm], b is the tube width [mm] and Γ is the Gamma function.

However, due to the irregularities in the shape of the deformed (flattened) cross-section of the bent tube, which occur in reality, it is usually not possible to effectively simplify the resulting cross-section as in Fig. 4. Therefore, still the most accurate method of ovality analysis remains the experimental determination or numerical simulation. It is important to note that the ovality is not uniform in the longitudinal tube direction, see Fig. 5. Based on the bending angle, the tube can be divided into 3 main areas: uniform oval area "A", uneven oval area "B" and undeformed area "C". The area "B" arises due to action of tools at both ends of the tube. In the uniform oval area "A", only the bending moment acts. Therefore, constant ovality of larger values can be expected here than in area "B". [Ghafoor 2001], [Miller 2001]

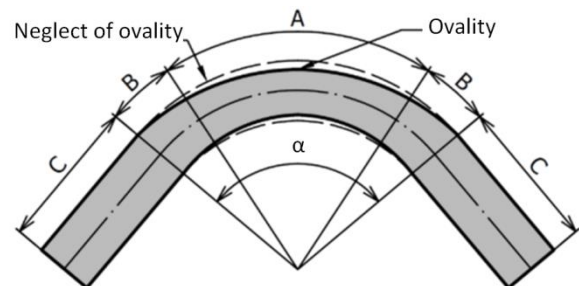


Figure 5. Uneven distribution of ovality [Srom 2017]

However, there are several methods to suppress ovality. Above all, the following are mainly used:

- axial compressive force,
- using of fillers,
- modification of the tool geometry.

Many authors have dealt with the tool modification in the past. An example of the possibilities of influencing the force action of tools on a bent tube according to [Wen 2014] is shown in Fig. 6. This approach represents a potential for improvement, which is not so much used in practice yet.

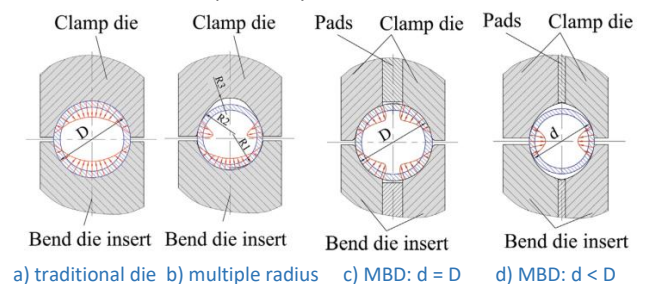


Figure 6. Action of contact force [Wen 2014]

Fig. 6 presents a universal tool, which is symmetrically divided and a pad is inserted between the die functional surfaces. The width of the pad depends on the bent diameter and it is adjusted as required. Fig. 6a means action of contact force in the traditional die. When the bend die with multiple radii is used, contact force effect is changed according to Fig. 6b. In the other figures, a multi-die body is considered (MBD).

2 EXPERIMENTAL DETERMINATION OF THE OVALITY

The tested bent part is a cold-drawn tube, which is made of 34MnB5 high-strength steel. Basic chemical composition and mechanical properties of mentioned steel according to tensile test results are presented in Tab. 1 and Tab. 2.

Yield stress	R_e	[MPa]	350
Ultimate strength	R_m	[MPa]	619
Young's modulus	E	[GPa]	191
Ductility	A_5	[%]	12.5

Table 1. Mechanical properties of 34MnB5 steel

%C	%Mn	%Si	%P	%S
0.33-0.37	1.2-1.4	0.15-0.30	max. 0.02	max. 0.005
%Al	%Ti	%Cr	%B	%Cu
0.02-0.05	0.02-0.05	0.10-0.18	0.0015-0.0035	max. 0.1

Table 2. Chemical composition of 34MnB5 steel

A tube with a diameter of 27 mm with a wall thickness of 3.2 mm is required to be bent by an angle of 120° over bending radius of 60 mm, see Fig. 7.

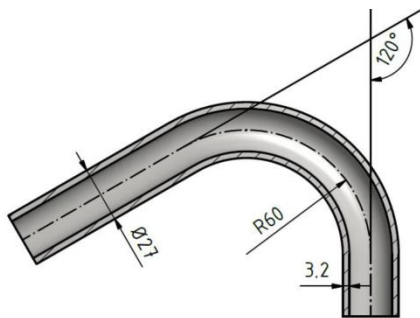


Figure 7. Required bend [Srom 2017]

The tube bending process was performed on Wafios RBV 60 ST CNC bending machine. The basic technical parameters of mentioned machine are summarized in Tab. 3.

Bending capacity		Maximal bending geometry parameters		Maximal speeds	
Bending torque	8 kNm	Tube diameter	35 mm	Advance feed	1 700 mm·s ⁻¹
Clamping force	140 kN	Feed length	3 500 mm	Rotation	450°·s ⁻¹
Boost pressure	50 kN	Bending angle	195°	Bending	180°·s ⁻¹

Table 3. Basic technical data of Wafios RBV 60 ST CNC bending machine

According to the possibilities of the machine, a tube with a total length of 1 500 mm was used for the experiments. The bending die rotated about the central axis with an angular velocity of 40° · s⁻¹. Guided end of the bent tube and the pressure bar move in a straight line in the axial direction with a length of 120.69 mm. A total of 6 identical bends were performed on the test tube, i.e. 6 specimens were obtained for experimental measurement of the ovality and possibly wall thinning of the formed tube, as it is shown in Fig. 8.

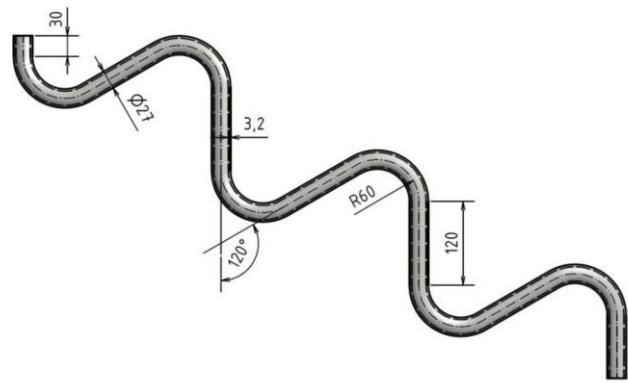


Figure 8. The specimen geometry [Srom 2017]

Each obtained specimen were cut after a bending angle step of 20° (see Fig. 9) and measured on an SSM-3E stereo microscope equipped with a USB camera. Measurement results were then averaged.

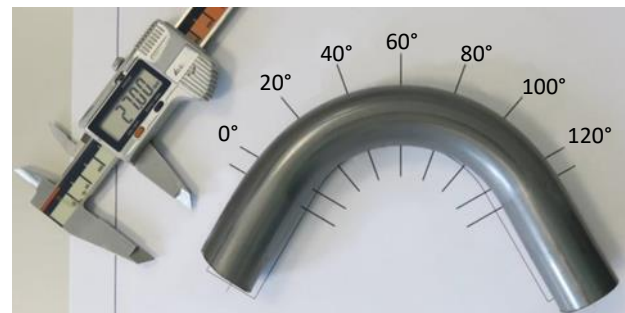


Figure 9. The bent specimen with sectional angles [Srom 2017]

The graph in Fig. 10 shows the average values of the detected ovality according to equation (1). The highest value was found for the sectional angle of 100°, namely 6.13 %. At this point, the cross-section changes in the radial direction to the axis of rotation from the original 27 mm to 25.32 mm (corresponds to D_{max} in Fig. 2). Cross-section change in the axial direction is almost unchanged (27.07 mm).

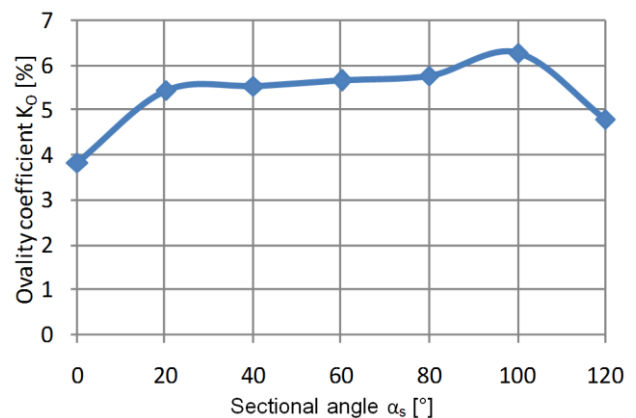


Figure 10. Detected change in the ovality

The detected minimal thickness of the individual cross-sections is shown in Fig. 11. Values in the graph correspond to the thinning of the cross-section on the outer side of the bent tube. The smallest value of the thickness has an angle of 100°, i.e. 2.88 mm, which corresponds to a reduction of 10 %.

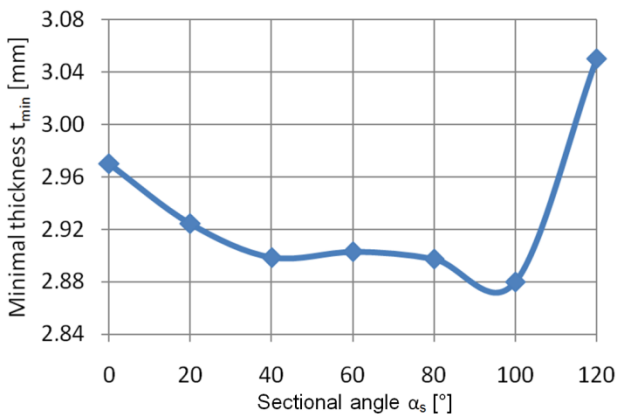


Figure 11. Detected change in minimal thickness

3 CHANGE OF THE PRESSURE DIE GEOMETRY

To improve the ovality status, a tool geometry is possible to change. In this case, the effort is to minimize the intervention of the bending process. Therefore, only the geometry of the pressure die has been modified. Obviously, there are a number of ways how to modify the pressure die geometry. The considered modifications are shown in Fig. 12.

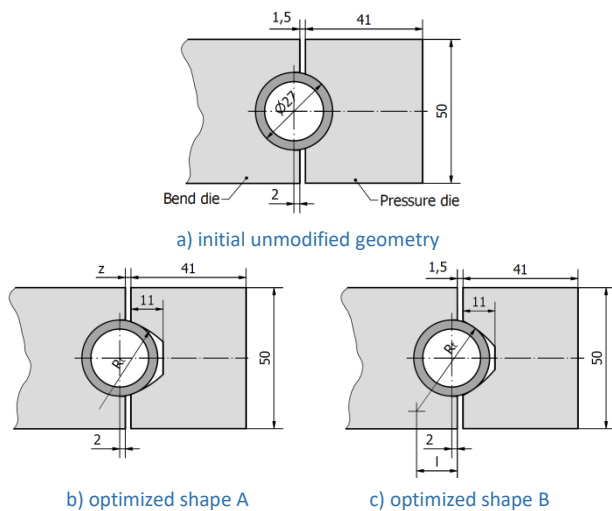


Figure 12. Optimized pressure die geometry

Proposed change in the pressure die geometry according to shape A counts with the replacement of the initial groove shape by a pair of curved surfaces (arcs) with a radius " R_t ". The arcs tangentially touch the bent tube. In addition to mentioned parameter, it is also possible to consider a different width of a gap between the bend die and the pressure die " z ".

Variant B also considers a pair of arcs with radius " R_t ". In this case, the distance from the axis of the bent tube " l " can be in addition change. This parameter can always obtain a different position of the contact points between the die and the tube groove. The gap between the bend die and the pressure die is kept the same as in the initial geometry, i.e. 1.5 mm.

In both cases, the proposed optimized shapes lead to a two-point contact between the tube and the pressure die in their cross-section, which should help to improve the ovality.

In the following, it is necessary to verify the functionality of the proposed shapes and find the optimal setting of the above mentioned geometric parameters for both variants. Therefore, an bending process analysis using a numerical simulation was performed.

4 NUMERICAL SIMULATION

For this purpose, the numerical simulation using the finite element method (FEM) in ANSYS Workbench 2020R2 software was used. Firstly, before the actual optimization, it is necessary to verify the correctness and accuracy of the theoretical model of numerical simulation by comparative simulation of the initial state.

A material model of the bent tube material, i.e. 34MnB5 steel, was determined according to tensile test data. Fig. 13 shows the final evaluated hardening curve plot. The tools were considered ideally rigid. For this reason, the definition of their material model is pointless. [Forejt 2004]

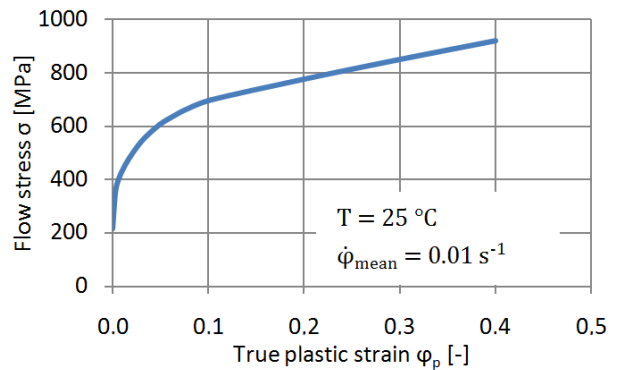


Figure 13. Flow stress of 34MnB5 steel

A friction condition was described according to the Coulomb's coefficient, which was set to 0.15. The geometric model was based on the description of the full 3D geometry of the tube, and the tools that are directly involved in its bending. The geometric model of the simulation after its discretization is shown in Fig. 14. For tube discretization, two hexaedral elements were used along the thickness.

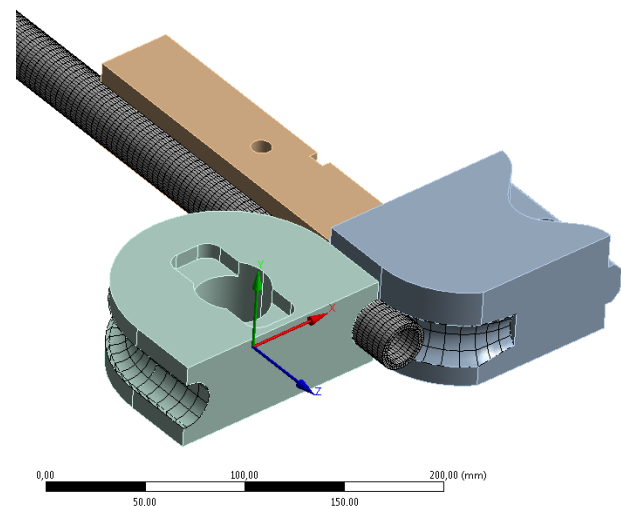


Figure 14. The FEM geometric model for rotary draw bending

Parameters of tool moves and rotations were then entered in accordance with the settings of the real experimental bend. The lateral pressure of the dies on the tube was originally set by a force. However, the force effect fluctuates depending on the resistances during the process in real manufacturing process. For better stability of simulation and better interpretation of results, the tools movement is controlled only by their position. A quasi-static analysis was used for the calculation. The speed of tool movement is thus not included in the calculation and also a possible strain rate effect was neglect.

4.1 Simulation with the Initial Geometry

After the calculation, it is possible to focus on simulation results for the verification of the simulation. Firstly, the experimentally determined ovality curves and the minimal wall thickness of the tube were compared with experimentally determined data, see Fig. 15 and Fig. 16.

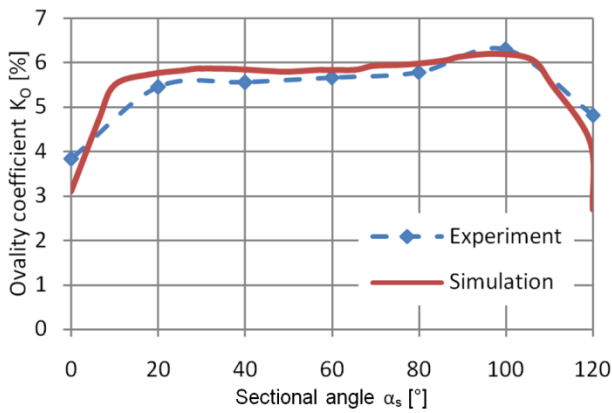


Figure 15. Comparison of change in the ovality

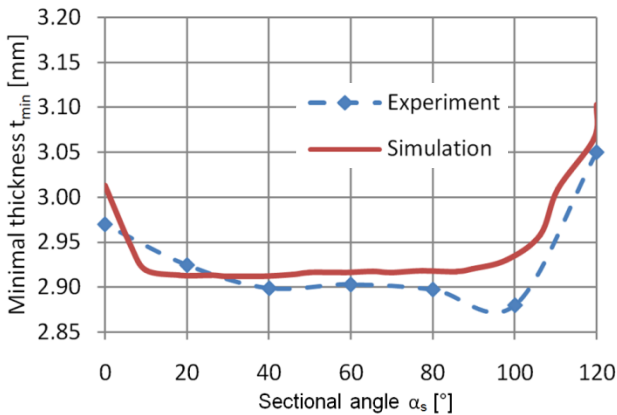


Figure 16. Comparison of change in minimal thickness

As can be seen in both graphs, the results show a quite good agreement between experimentally measured and numerically calculated data. However, in marginal areas of the monitored angle there are significant differences in the comparison of the monitored ovality and minimal thickness. These differences can be probably caused by simplified boundary conditions of the FEM simulation. Besides the above, in the graph of Fig. 16, more substantial differences can be observed for the sectional angle of 100°, but which is only about 2 %.

Another way how to verify the numerical simulation is to compare the change in the tube cross-section geometry. Fig. 17 shows an example of a comparison for bending angle of 100°, i.e. in the most problematic place in terms of ovality and thinning.

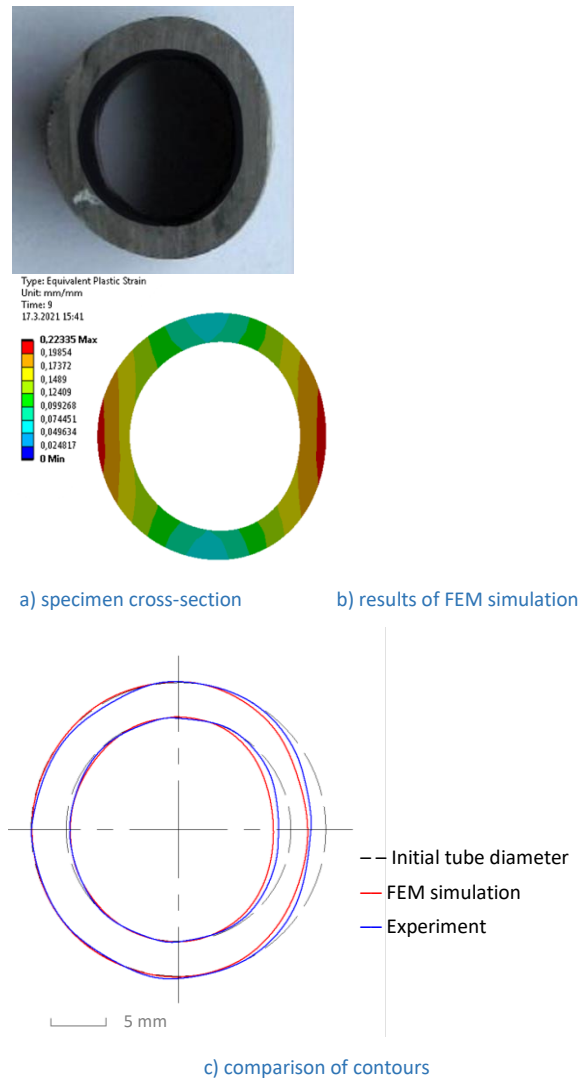


Figure 17. Comparison of the deformed cross-section geometry

As it is clearly evident from the Fig. 17, the geometry, which is predicted by the simulation, is very close to the experimentally determined shape with a deviation not exceeding 0.62 mm. It is possible to note that the simulation almost coincides with real geometry and it is convenient in terms of verification. In the following, it is therefore possible to use FEM analysis to verify the proposed pressure die geometries.

4.2 Simulation of the Proposed New Geometry

Both optimized shape variants from Fig. 12 was analyzed by FEM simulation and the comparison with initial unmodified pressure die geometry was performed. Simulation results are presented below.

Firstly, the variant of shape A was investigated. As it was mentioned before, there are two main geometric parameters that were changed for individual variants. The radius "R_t" was examined in the range of 15 to 80 mm. Gap between the bend die and the pressure die "z" was gradually changed from initial value of 1.5 mm to 4 mm. For combinations of these parameters, the curves of change in the ovality coefficient as a function of sectional angle are shown in Fig. 18 to Fig. 20 below.

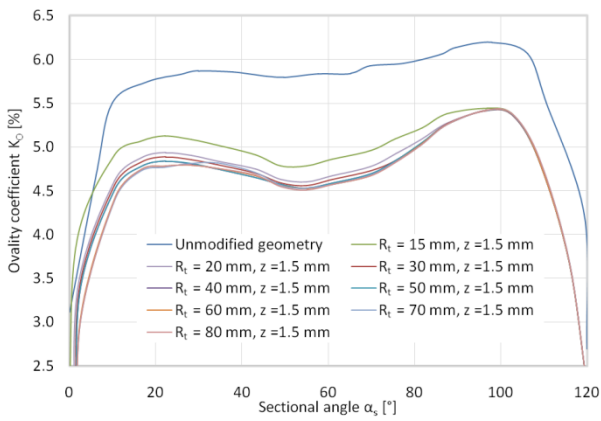


Figure 17. Change in the ovality for shape A with $z = 1.5$ mm

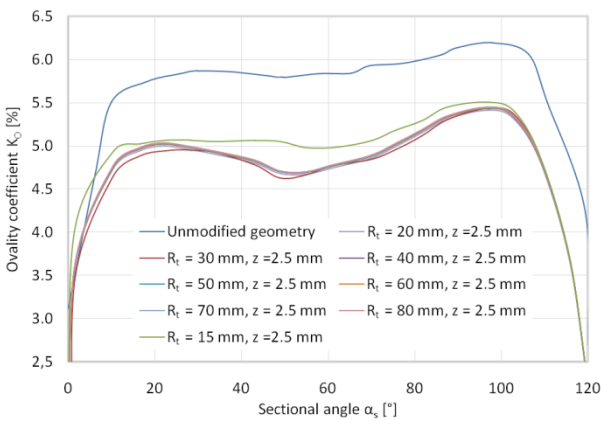


Figure 18. Change in the ovality for shape A with $z = 2.5$ mm

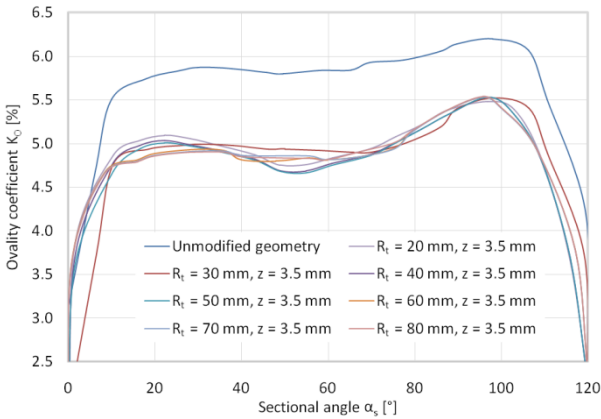


Figure 19. Change in the ovality for shape A with $z = 3.5$ mm

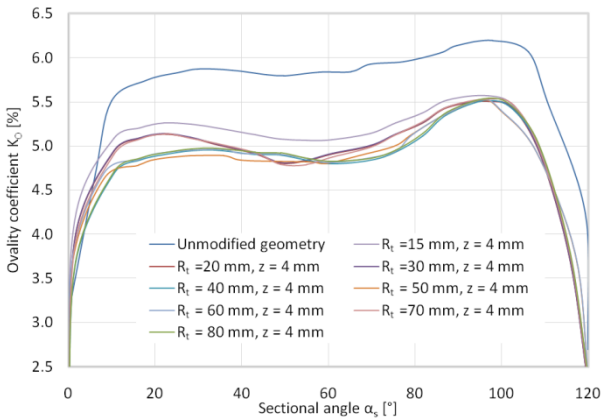


Figure 20. Change in the ovality for shape A with $z = 4$ mm

The comparison clearly shows that the modification of the geometry clearly leads to an improvement in ovality, for all variants. The improvement is not great. Nevertheless, an improvement in the order of 10 to 12 % can be observed in comparison with the initial die geometry. The individual variants seem to be more or less equivalent. Although, in terms of the maximum ovality achieved, the best results are achieved with a variant with the radius of $R_t = 20$ mm and the gap $z = 2.5$ mm. A closer comparison of the maximal values of the ovality coefficient for individual variants is summarized in Fig. 21. The graph in Fig. 22 provides an overview of the minimum improvement achieved in the ovality coefficient.

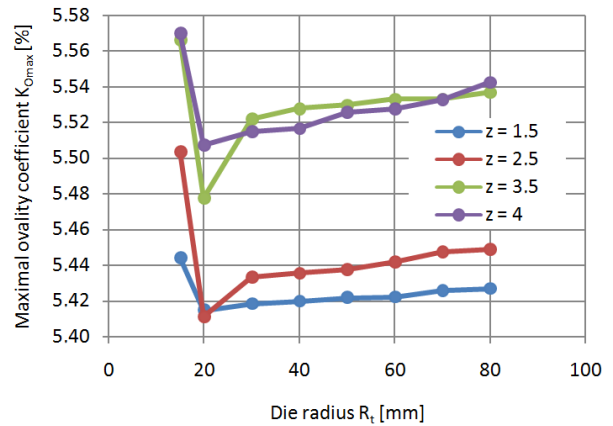


Figure 21. Change in the maximal value of the ovality coefficient for shape A

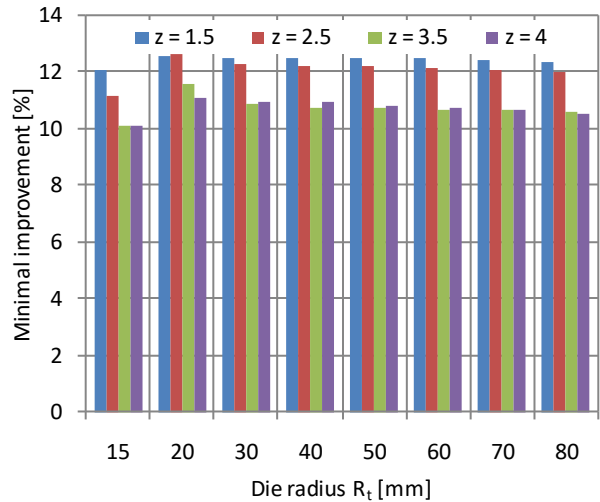


Figure 22. Minimal improvement of individual variants for shape A

The same evaluation method can be used in the case of the shape B, see Fig. 12c. In this case, parameters, such as the die radius " R_t " and the distance between center point of the die radius and the axis of the bent tube " l ", was change for individual analyzed variants. Parameter " R_t " was set from a range of 20 to 60 mm. " l " values were different for each radius, because a variable die radius brings a different position of its center point. Curves of change in the ovality coefficient are shown in Fig. 23 to Fig. 26.

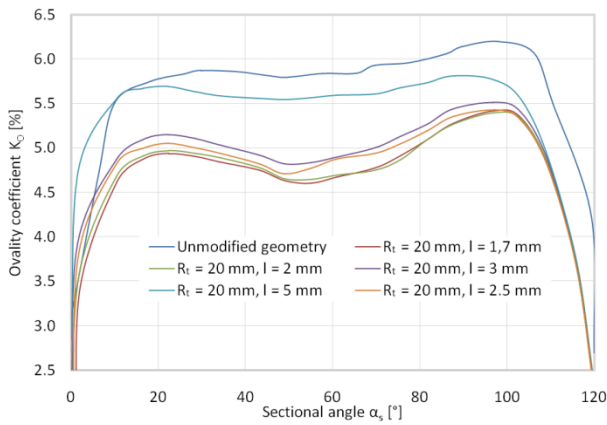


Figure 23. Change in the ovality for shape B with $R_t = 20$ mm

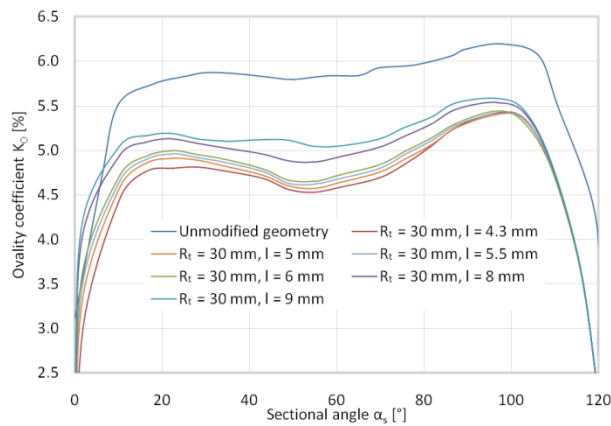


Figure 24. Change in the ovality for shape B with $R_t = 30$ mm

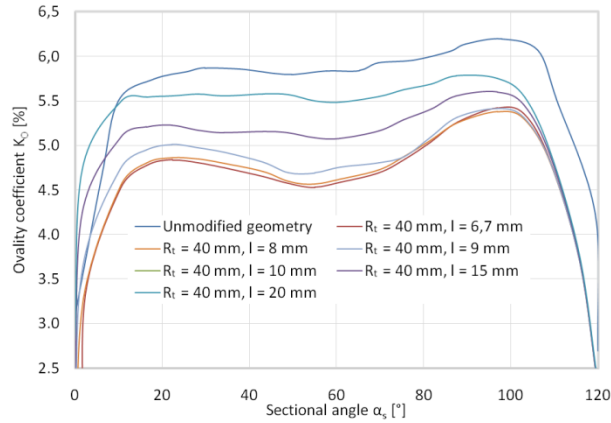


Figure 25. Change in the ovality for shape B with $R_t = 40$ mm

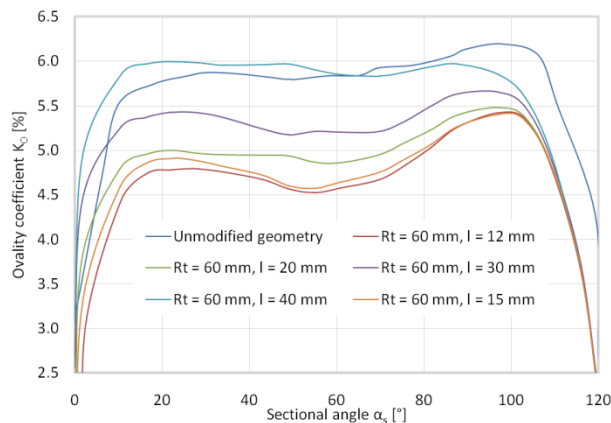


Figure 26. Change in the ovality for shape B with $R_t = 60$ mm

It is clearly evident that even in this case, the modification of the geometry of the pressure bar achieves a noticeable improvement in ovality compared to the current state. A wide range improvement in the order of 3.2 to 13.3 % can be observed. In term of the maximum ovality achieved, the variant of $R_t = 40$ mm with $l = 8$ mm shows the best results, see Fig. 27. This fact is also confirmed by a clearer summary of the percentage improvement in the ovality coefficient in Fig. 28.

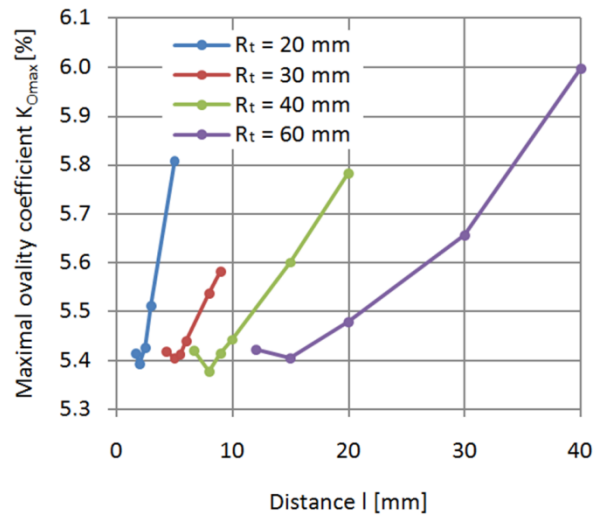


Figure 27. Change in the maximal value of the ovality coefficient for shape B

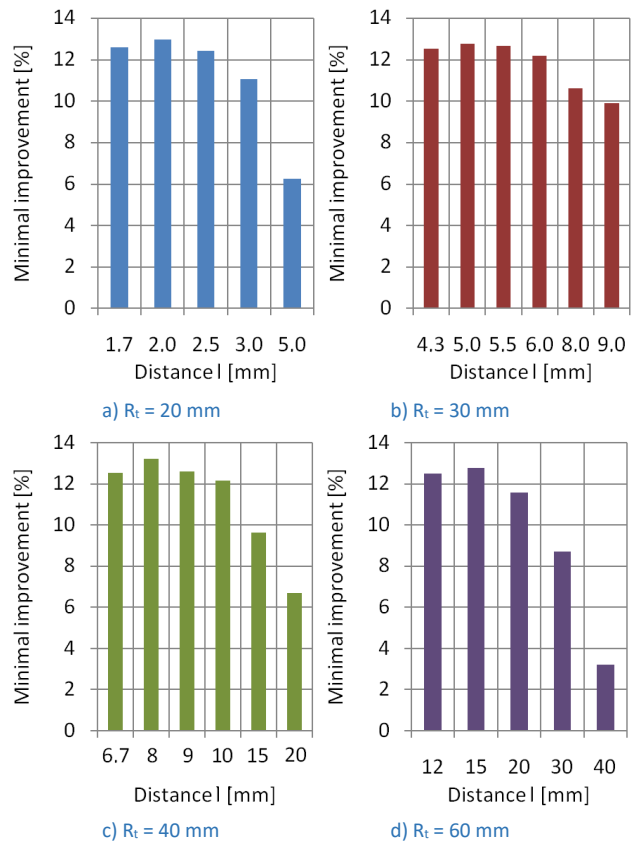


Figure 28. Minimal improvement of individual variants for shape B

5 RESULTS AND DISCUSSION

If all tested variants are compared across both shapes (A and B), it is clear that many of them are almost identical over the course of the determined ovality coefficient. In some cases, they differ

from each other only in the order of hundredths of percent. Nevertheless, there is an effort to select the optimal variant of geometry modifications of the pressure bar. From the point of view of the maximal achieved value of the ovality coefficient, shape B with set parameters $R_t = 40$ mm and $t = 8$ mm seems to be the most suitable. The smallest improvement of 13.2 % is achieved here. However, it should be mentioned that also some other modifications achieve similar results, namely for shape B of the variant $R_t = 20$ mm with $l = 2$ mm or $R_t = 15$ mm with $l = 15$ mm. From shape A, the variant with the radius $R_t = 20$ mm and the gap $z = 2.5$ mm achieves comparable results too. None of them achieve such an improvement as the previously mentioned shape B variant. An overview of the percentage expression of ovality improvement for this variant in the whole examined range of α is further summarized in tab.

Angle α_s [°]	Ovality coefficient K_o [%]		Improvement [%]
	Initial geometry	Shape B	
0	3.115	1.459	53.154
20	5.780	4.863	15.866
40	5.837	4.711	19.289
60	5.837	4.626	20.748
80	5.986	5.056	15.544
100	6.196	5.378	13.206
120	2.693	2.241	16.794

Table 4. Improvement of the ovality coefficient (Shape B, $R_t = 40$ mm, $l = 8$ mm)

The deformed cross-section of the bent tube for the best variant of the pressure die geometry ($R_t = 40$ mm, $l = 8$ mm) is for various sectional angles shown in Fig. 29. Furthermore, the figure also shows the distribution of the plastic strain along the cross-section. It can be noted that the largest deformation occurs on the sides of the bent cross-section, in the range $\alpha_s = 20^\circ$ to 100° with the greatest ovality at 100° .

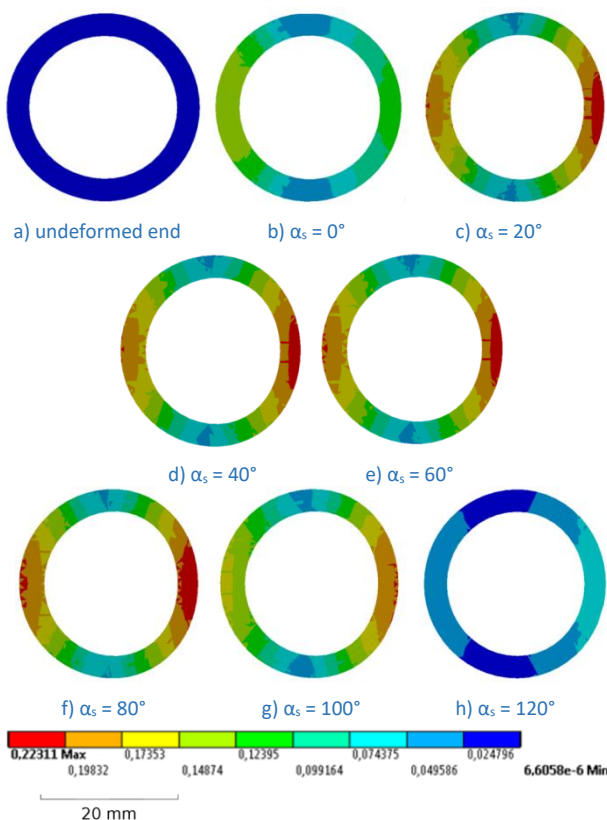


Figure 29. Distribution of plastic strain on deformed cross-section geometry

6 CONCLUSIONS

The article was focused on the influence of the modification of the pressure bar geometry on the resulting ovality of the formed tube, which was bent to a bending radius of 60 mm by an angle of 120° using the rotary draw bending method on Wafios RBV 60 ST CNC bending machine. A tube that is made of 34MnB5 steel with the diameter of 27 mm and the wall thickness of 3.2 mm was used for experimental evaluation.

Overall, two modifications of the pressure bar geometry were considered, i.e. shapes A and B. The influence of the modified geometric tools on the resulting ovality was assessed on the basis of the numerical simulation in the ANSYS Workbench 2020 R2 software. Before the actual numerical analysis, the accuracy of the simulation was experimentally verified by the comparison with the initial tool geometry. Subsequently, a set of numerical simulations was performed for various variants of considered shapes.

It is clear from the simulation results that the modification of the die geometry makes sense. Although in this case, one of the bending tools was modified, moreover without considering the modification of the pressing or boosting force, both proposed variants achieve a significant improvement in the detected ovality coefficient. In the case of optimized shape B with parameters $R_t = 40$ mm and $l = 8$ mm, improvement reaches values of at least 13.3 % for sectional angle 100° . The maximal improvement exceeds 50 % for the outer of the observed bending angle.

Due to the fact that the article focuses only on the change of the geometry of the pressure bar, in the future it is possible to focus on other possibilities and its combination, such as the change of the already mentioned pressure force, etc.

ACKNOWLEDGMENTS

The paper was supported by project "Analysis of formability and weldability of materials produced by 3D wire metal printing" within the specific research of Faculty of Mechanical Engineering, Brno University of Technology relating to the grant no. FSI-S-20-6336.

REFERENCES

- [Forejt 2004] Forejt, M. et al. Establishing the dynamic mechanical properties of materials by the hopkinson test method. Acta Mechanica Slovaca, 2004, Vol. 8, No. 2b, pp 93-98, ISSN: 1335-2393
- [Ghafoor 2001] Ghafoor, K. How material influences bending for hydroforming: Effects on ovality, spring-back, and wall thickness in tubes. The Tube & Pipe Journal, 2001, Vol. 4, No. 1, pp 50-119, ISSN 0162-9700
- [Miller 2001] Miller, J. E. et al. On bend stretch forming of aluminum extruded tubes - I: experiments. International Journal of Mechanical Sciences, 2001, Vol. 43, No. 5, pp 1591-1599, ISSN 0020-7403
- [Li 2010] Li, H. et al. Deformation behaviors of thin-walled tube in rotary draw bending under push assistant loading conditions.

Journal of Materials Processing Technology, 2010, Vol. 210, No. 1, pp 143-158, ISSN 0924-0136

[Liu 2011] Liu, Y. and Daxin, E. Effects of cross-sectional ovalization on springback and strain distribution of Circular tubes under bending. Journal of Materials Engineering and Performance, 2011, Vol. 20, No. 9, pp 1283-1317, ISSN 1059-9495

[Safdarian 2019] Safdarian, R. Investigation of tube fracture in the rotary draw bending process using experimental and numerical methods. Journal of Material Forming, 2019, Vol. 13, No. 4, pp 493-516, ISSN 1960-6206

[Srom 2017] Srom, J. Analysis of Tube Bending Process. Brno: Brno University of Technology, 2020. (In Czech)

[Tang 2000] Tang, N. C. Plastic-deformation analysis in tube bending. International Journal of Pressure Vessels and Piping, September 2000, Vol. 77, No. 12, pp 751-759, ISSN 0308-0161

[Welo 2015] Welo, T. and Paulsen, F. Predicting Tube Ovalization in Cold Bending: An Analytical Approach. Key Engineering Materials, July 2015, Vol. 651, No. 1, pp 1146-1152, ISSN 0308-0161

[Wen 2014] Wen, T. On a new concept of rotary draw bend-die adaptable for bending tubes with multiple outer diameters under non-mandrel condition. Journal of Materials Processing Technology, 2014, Vol. 214, No. 2, pp 311-317, ISSN 0924-0136

CONTACTS:

Ing. Jan Rihacek, Ph.D., Ing. Michaela Cisarova, Ph.D., Ing. Eva Peterkova, Ph.D., Ing. Kamil Podany, Ph.D.
Brno University of Technology, Faculty of Mechanical Engineering, Institute of Manufacturing Technology, Department of Metal Forming
Technicka 2896/2, Brno, 616 69, Czech Republic
e-mail: rihacek.j@fme.vutbr.cz